Isolation and sequence analysis of the peptide antibiotics trichorzins PA from *Trichoderma harzianum*

Delphine Duval,[a] Sylvie Rebuffat,*[,a] Christophe Goulard,[a] Yann Prigent,[b] Michel Becchi[c] and Bernard Bodo[a]

[a] *Laboratoire de Chimie des Substances Naturelles, URA 401, GDR 1153 CNRS, IFR 63 CNRS-INSERM, Muséum National d'Histoire Naturelle, 63 rue Buffon, 75231 Paris Cedex 05, France*
[b] *Laboratoire de RMN, URA 464 CNRS, IFR MP 23 INSERM, Université de Rouen, 76821 Mont-Saint-Aignan Cedex, France*
[c] *Service Central d'Analyse du CNRS, Laboratoire de Spectrométrie de Masse, Echangeur de Solaize, BP 22, 69390 Vernaison, France*

Trichorzins PA are new members of the class of natural Aib-containing peptides, which are known under the common name peptaibols. They are produced by a *Trichoderma harzianum* strain and exhibit significant activity against mycoplasmas. From the natural peptide mixture, seven trichorzins PA (PA II and IV–IX) have been isolated by a procedure employing different chromatography steps and a final purification by reversed-phase HPLC. The amino acid sequence elucidation involved a combination of liquid secondary-ion mass spectrometry (LSIMS) and two-dimensional ^{1}H and ^{13}C NMR spectroscopy. Trichorzins PA are 18-residue peptaibols which differ mainly from other, related peptides by the *C*-terminal amino alcohol which is either tryptophanol or phenylalaninol. They adopt a helical structure.

Introduction

Peptaibols, which are linear hydrophobic peptides produced by *Trichoderma* soil fungi and exemplified by alamethicin,[1] inhibit the growth of a number of Gram positive bacteria, such as *Staphylococcus aureus*. The antimicrobial action is strongly related to cytoplasmic membrane perturbation. Organised in amphipathic helices, peptaibols interact with phospholipid bilayers and increase their permeability, either in the presence [2,3] or in the absence of an applied voltage.[3,4] The voltage-dependent channel-forming property has been suggested to result from transbilayer helix bundles formed by assembly of amphiphilic peptide monomers.[3,5,6] Peptaibols are characterised by an acetylated *N*-terminus, a high content in α-aminoisobutyric acid (Aib) and a *C*-terminal amino alcohol. They contain either 18–20 residues (long-sequence peptaibols [1,7–9]) or 7–16 residues (short-sequence peptaibols [10–12]) and lipopeptaibols [13,14].

A mixture of original peptaibols termed trichorzins PA was isolated from a *Trichoderma harzianum* strain selected for its antagonistic properties toward other microorganisms. The trichorzin PA mixture was shown to exert potent activity against *Mycoplasma* and *Spiroplasma* cells and, as expected, against *S. aureus*. Known as the smallest and simplest self-replicating prokaryotes and members of the class mollicutes, *Mycoplasma* and *Spiroplasma* cells hold the record for the smallest genome and are auxotrophs for many metabolites.[15,16] They are thus parasites of humans, animals, arthropods and plants and many species are pathogens and develop resistance to commercial antibiotics. The peptides isolated from the natural trichorzin microheterogeneous mixture were found to inhibit the growth of *Mycoplasma*, *Spiroplasma* and *Acholeplasma* cells with MIC values ranging between 3 and 25 μM. For comparison, alamethicin, a well known 20-residue peptaibol, and the bee venom melittin had MIC values in the same range, between 1.5 and 12.5 μM.[17]

We now report the production, isolation and sequence determination of trichorzins PA II and IV–IX, seven new 18-residue peptaibols from *T. harzianum*. The influence on the peptide conformation of the slight sequence modifications leading to the trichorzin PA microheterogeneity is discussed.

Results and discussion

1 Isolation and HPLC separation of trichorzins PA

Fermentation of *T. harzianum* (strain M-902608) on liquid synthetic medium gave rise to a peptide mixture, extracted from culture broth and mycelium with butan-1-ol and methanol, respectively. Crude peptide mixtures were obtained from the two extracts by exclusion chromatography through Sephadex LH 20. In both cases, further silica gel chromatography afforded three peptide groups of increasing polarities PC, PA and PB; the PB and PC groups were complex mixtures of short-sequence peptides. When analysed by reversed-phase HPLC, the trichorzin PA group appeared as a mixture of at least 11 peptides from which nine components, PA I–IX (Fig. 1) were isolated by repetitive semi-preparative HPLC and further analysed. Trichorzins PA I and PA III still appeared as mixtures of at least two homologous peptides; trichorzins PA II and PA

		1	2	3	4	5	6	7	8	9	10	11	12	13	14	15	16	17	18
PA II	Ac	Aib	Ser	Ala	**Aib**	Iva	Gln	**Aib**	Val	Aib	Gly	Leu	Aib	Pro	Leu	Aib	Aib	Gln	**Trpol**
PA IV	Ac	Aib	Ser	Ala	**Aib**	Iva	Gln	**Iva**	Val	Aib	Gly	Leu	Aib	Pro	Leu	Aib	Aib	Gln	**Trpol**
PA V	Ac	Aib	Ser	Ala	**Iva**	Iva	Gln	**Aib**	Val	Aib	Gly	Leu	Aib	Pro	Leu	Aib	Aib	Gln	**Trpol**
PA VI	Ac	Aib	Ser	Ala	**Aib**	Iva	Gln	**Aib**	Val	Aib	Gly	Leu	Aib	Pro	Leu	Aib	Aib	Gln	**Pheol**
PA VII	Ac	Aib	Ser	Ala	**Iva**	Iva	Gln	**Iva**	Val	Aib	Gly	Leu	Aib	Pro	Leu	Aib	Aib	Gln	**Trpol**
PA VIII	Ac	Aib	Ser	Ala	**Aib**	Iva	Gln	**Iva**	Val	Aib	Gly	Leu	Aib	Pro	Leu	Aib	Aib	Gln	**Pheol**
PA IX	Ac	Aib	Ser	Ala	**Iva**	Iva	Gln	**Aib**	Val	Aib	Gly	Leu	Aib	Pro	Leu	Aib	Aib	Gln	**Pheol**

Sequences of trichorzins PA (Bold letters indicate those amino acids which differ in the sequences)

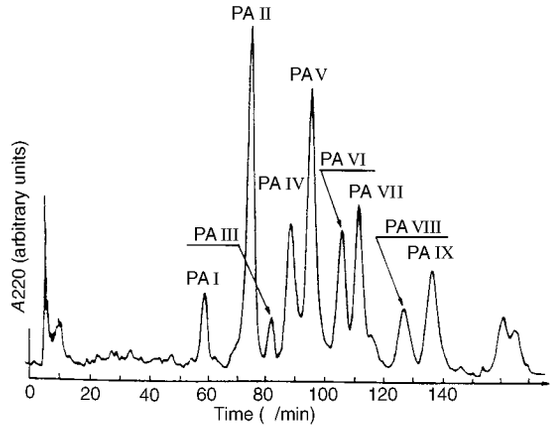

Fig. 1 HPLC elution profile of trichorzins PA from *T. harzianum* M-902608; Kromasil C_{18} (5 μm), 7.5 × 300 mm, MeOH–water (83 : 17), flow rate 2 cm^3 min^{-1}, absorption monitored at 220 nm

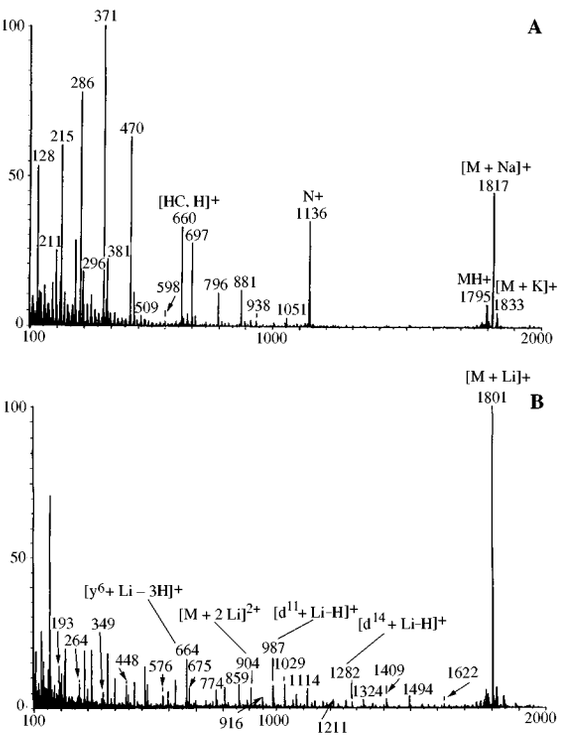

Fig. 2 Positive-ion LSI mass spectra of PA VIII with two different matrices; **A**: 3-nitrobenzyl alcohol; **B**: 3-nitrobenzyl alcohol saturated with LiCl

IV–IX were single peptides and were submitted to sequence analysis.

Trichorzins PA gave a negative reaction with ninhydrin, revealing the absence of free NH_2-terminal groups; sharp singlets at ~2.0 ppm observed in the 1D ^{1}H NMR spectra indicated the *N*-terminal residues to be acetylated. The spectra of PA II, IV, V and VII showed characteristic aromatic proton spin systems together with singlets at δ ~10.2, which supported the presence of an indolic group. Tryptophanol was actually characterised in the mercaptoethanesulfonic acid hydrolysates of these peptides. Complete amino acid composition and absolute configuration arose from GLC analysis of the total acidic hydrolysates after derivatisation and comparison with standards. Chirality of the monoalkylated amino acids and amino alcohols (phenylalaninol or tryptophanol) was L, while that of isovaline was D. Finally, the L-Glx residues were assigned to L-Gln from the absence of any acidic function in the peptides and from observation of the *syn* and *anti* ε-protons of the carboxamide groups in the ^{1}H NMR spectra.

2 Sequence determination of trichorzins PA

a LSI MS data. Positive-ion fast-atom bombardment (FAB) and liquid secondary-ion (LSI) mass spectrometry proved useful in the sequence determination of peptides[18–20] and particularly of peptaibols.[8,9,11–14,21,22] Spectra were obtained for the pure isolated PA using three different matrices, either α-thioglycerol, 3-nitrobenzyl alcohol or 3-nitrobenzyl alcohol saturated with LiCl, in order to perform peptide cationisation. The mass spectra of trichorzins PA II and PA IV–IX appeared to be relatively similar and indicated that the compounds were single peptides, differing in their sequence only by one to three amino acids. Trichorzin PA VIII was taken as an example: the spectra obtained in the presence of either 3-nitrobenzyl alcohol (Fig. 2A) or α-thioglycerol as matrix displayed a similar fragmentation pattern, while it completely differed in the presence of Li^+ (Fig. 2B).[23] This was also observed for the other trichorzins PA.

The molecular masses were determined from the molecular ion species, either MH^+, $[M + Na]^+$ and $[M + K]^+$ in the absence of added lithium, or $[M + Li]^+$ and $[M + 2Li]^{2+}$ in the presence of lithium (Tables 1 and 2). As previously observed in the absence of LiCl for other peptaibols, the most important fragmentations of trichorzins PA were amide bond cleavages leading to b_n acylium ions,[8,9,11–14,21,22] whereas $[a_n + Li - H]^+$ ions were mainly detected when adding LiCl.[23] The mass difference between two consecutive ions of the same series allowed sequence determination. The preferential cleavage at the Aib-Pro bond, giving rise to the formation of complementary *N*-terminal acylium N^+ ion and *C*-terminal diprotonated ammonium $[HC,H]^+$ ion (Table 1), which is typical of peptaibols containing Aib-Pro bonds, did not prevail in the presence of lithium (Table 2). The spectra obtained with the lithiated adducts each showed a single series of $[a_n + Li - H]^+$ ions, starting from the lithiated adduct ions[23–25] and accompanied in some cases by $[d_n + Li - H]^+$ ions which arose from the loss of a radical from the side chains, as a result of β-cleavage. Such ions can differentiate between the isomeric Leu/Ile residues, from the mass differences between the $[a_n + Li - H]^+$ and the corresponding $[d_n + Li - H]^+$ ions (Leu and Ile are characterised by such differences of 42 a.m.u. and 28 a.m.u., respectively). These ions here confirmed the presence of two leucines at positions 11 and 14 in the PA sequences. Fig. 3 shows the typical fragmentation pattern of trichorzin PA VIII, taken as an example.

The sequences of trichorzins PA were thus determined in this way, except for the respective location of the isomeric Val/Iva.

b ^{1}H, ^{13}C and ^{15}N NMR data. Complete sequential ^{1}H assignments and sequence determination of trichorzins PA were obtained in two steps, according to the method previously developed by Wüthrich.[26] At first, chemical shifts for the different amino acid types were assigned by the use of ^{1}H–^{1}H chemical-shift correlation (COSY) and two-dimensional total correlation spectroscopy (TOCSY) experiments, then contiguous residues were connected through rotating-frame nuclear Overhauser enhanced (ROE) data, affording their sequential position. Those data also led to stereospecific assignments and conformational features. Furthermore, ^{13}C and ^{15}N sequential assignments arose from heteronuclear single-quantum coherence (HSQC) and heteronuclear multiple-bond correlation (HMBC) experiments.

The ^{1}H spectrum amide proton region of PA VI (Fig. 4) exhibited 8 singlets corresponding to the Aib and Iva α-dialkylated residues in addition to one triplet characterising a glycine and to 8 doublets. The COSY experiment provided scalar connectivities between the amide proton of each monoalkylated residue and its α proton. The assigned signals were further correlated to the lateral chain protons by both COSY and TOCSY data (Fig. 4), allowing us to describe the characteristic spin systems (Tables 3 and 4).

Table 1 Pseudomolecular ion species and sequence-specific fragment ions arising in the (+) ion LSI mass spectra of trichorzins PA (H = 1.000); 3-nitrobenzyl alcohol as matrix; the origin of the observed ions, from N^+ or $[HC, H]^+$ is indicated by *N* or *C*, respectively

	Peptides	PA II 1819 $C_{86}H_{141}N_{21}O_{22}$		PA IV 1833 $C_{87}H_{143}N_{21}O_{22}$		PA V 1833 $C_{87}H_{143}N_{21}O_{22}$		PA VI 1780 $C_{84}H_{140}N_{20}O_{22}$		PA VII 1847 $C_{88}H_{145}N_{21}O_{22}$		PA VIII 1794 $C_{85}H_{142}N_{20}O_{22}$		PA IX 1794 $C_{85}H_{142}N_{20}O_{22}$	
Ion types		*m/z*	%	*m/z*	%	*m/z*	%	*m/z*	%	*m/z*	%	*m/z*	%	*m/z*	%
$[M + K]^+$		1858	11	1872	13	1872	3	1819	7	1886	2	1833	5	1833	14
$[M + Na]^+$		1842	100	1856	80	1856	16	1803	47	1870	14	1817	43	1817	45
MH^+		1820	19	1834	11	1834	4	1781	10	1848	1	1795	7	1795	16
N^+	b^{12}	1122	9	1136	32	1136	22	1122	36	1150	14	1136	35	1136	44
$[HC, H]^+$	y^6	699	7	699	13	699	30	660	40	699	12	660	33	660	43
N	b^{11}	1037	1	1051	3	1051	2	1037	3	1065	1	1051	3	1051	4
N	b^{10}	929	1	938	2	938	2	924	2	952	1	938	2	938	3
N	b^9	867	4	881	12	881	9	867	10	895	7	881	11	881	12
N	b^8	782	3	796	11	796	7	782	8	810	7	796	10	796	11
N	b^7	683	8	697	29	697	22	683	24	711	16	697	27	697	25
N	b^6	598	1	598	2	612	1	598	1	612	2	598	1	612	2
C		509	2	509	3	509	5	509	4	509	5	509	3	509	5
N	b^5	470	19	470	60	484	51	470	55	484	47	470	63	484	57
C		381	4	381	6	381	11	381	10	381	12	381	8	381	10
N	b^4	371	38	371	100	385	94	371	100	385	76	371	100	385	100
C		296	7	296	11	296	22	296	19	296	22	296	17	296	19
N	b^3	286	32	286	65	286	87	286	79	286	100	286	78	286	76
N	b^2	215	26	215	43	215	87	215	83	215	66	215	60	215	84
C		211	5	211	8	211	18	211	16	211	16	211	14	211	16
N	b^1	128	25	128	25	128	100	128	88	128	68	128	53	128	90

Table 2 Pseudomolecular ion species and sequence-specific fragment ions arising in the (+) ion LSI mass spectra of trichorzins PA (H = 1.000); 3-nitrobenzyl alcohol saturated with LiCl as matrix

Peptides	PA IV		PA VII		PA VIII		PA IX	
Ion types	*m/z*	%	*m/z*	%	*m/z*	%	*m/z*	%
$[M + Li]^+$	1840	100	1854	100	1801	100	1801	100
$[M + 2Li]^{2+}$	924	3	931	19	904	7	904	16
$[a^{17} + Li - H]^+$	1622	6	1636	1	1622	1	1622	2
$[a^{16} + Li - H]^+$	1494	12	1508	2	1494	3	1494	5
$[a^{15} + Li - H]^+$	1409	10	1423	13	1409	3	1409	5
$[a^{14} + Li - H]^+$	1324	10	1338	1	1324	3	1324	5
$[a^{13} + Li - H]^+$	1211	8	1225	13	1211	3	1211	4
$[a^{12} + Li - H]^+$	1114	17	1128	25	1114	6	1114	12
$[a^{11} + Li - H]^+$	1029	17	1043	25	1029	8	1029	14
$[a^{10} + Li - H]^+$	916	1	930	13	916	1	916	4
$[a^9 + Li - H]^+$	859	11	873	25	859	8	859	14
$[a^8 + Li - H]^+$	774	10	788	25	774	6	774	10
$[a^7 + Li - H]^+$	675	9	689	25	675	7	675	10
$[a^6 + Li - H]^+$	576	6	590	25	576	4	590	9
$[a^5 + Li - H]^+$	448	5	462	25	448	4	462	10
$[a^4 + Li - H]^+$	349	3	363	31	349	3	363	10
$[a^3 + Li - H]^+$	264	4	264	44	264	4	264	9
$[a^2 + Li - H]^+$	193	5	193	56	193	6	193	10
$[a^1 + Li - H]^+$	106	6	106	56	106	1	106	9
$[d^{11} + Li - H]^+$	987	19	1001	25	987	7	987	14
$[d^{14} + Li - H]^+$	1282	8	1296	1	1282	2	1282	4
$[y^6 + Li - 3H^+]$	703	6	703	28	664	16	664	28

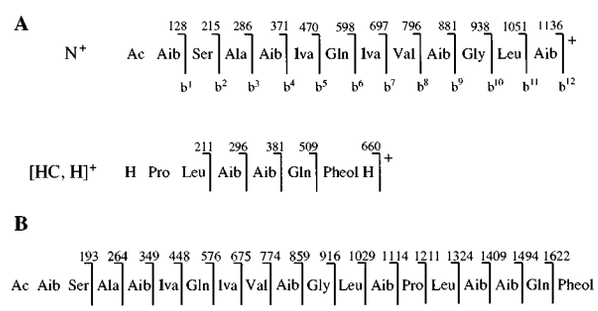

Fig. 3 **A**. Mass fragmentation pattern of PA VIII exhibiting the sequence-specific fragment ions of the N^+ and $[H,CH]^+$ ions; **B**. Mass fragmentation pattern of PA VIII under cationisation by Li^+ ions, exhibiting the series of sequence-specific $[a_n + Li - H]^+$ ions.

The ROE inter-residue correlations between contiguous residues, such as $d_{\mathbf{NN}(i,\ i+1)}$ and $d_{\alpha N(i,\ i+1)}$, led to complete sequential information. Two sequence parts, from residues 1 to 12 and 14 to 18, were assigned from the two series of $d_{\mathbf{NN}(i,\ i+1)}$ correlations, interrupted only by the lack of an amide proton at proline 13 (Fig. 5). They were connected by $d_{\alpha N(i,\ i+1)}$ between the Pro[13] α-proton and the Leu[14] amide. The Iva and Val isomeric residues in the PA VI sequence were thus located at positions 5 and 8, respectively. The sequences of the other isolated PAs were completed in the same way.

Taking into account the *S* configuration of the α carbon, the proline stereospecific assignments were obtained from the intra-residue dipolar correlations between Hα, *pro-S* Hβ, *pro-R* Hγ and *pro-R* Hδ which showed that these protons were all located on the same side of the ring.

Complete ^{13}C assignments of the amino acid lateral chains resulted from the $^1J_{\mathbf{CH}}$ connectivities observed in the ^1H–^{13}C HSQC spectra. Quaternary carbons, such as carbonyl groups and Aib α carbons, were assigned with the aid of ^1H–^{13}C HMBC correlations optimised for $J_{\mathbf{CH}}$ long-range couplings (5

Table 3 ^{1}H, ^{13}C and ^{15}N chemical shifts for trichorzin PA VI (CD_3OH; 298 K)

	^{1}H			^{13}C			^{15}N
Residue	NH	H^{α}	Other groups (*J*, Hz)	CO	Cα	Other groups	NH
Ac			Me 2.055	173.5		Me 22.9	132.9
U[1]	8.575		Me β1 1.487/Me β2 1.491	178.1	58.0	Me β1 23.2/Me β2 26.4	102.3
S[2]	7.988	4.18	β 3.89/β′ 3.95	173.5	59.2	β 61.8	118.5
A[3]	7.901	4.19	β 1.47	176.4	53.3	Me β 16.2	122.7
U[4]	7.795		Me β1 1.476/Me β2 1.552	176.4		Me β1 23.0/Me β2 26.5	113.9
J[5]	7.602		β1 1.76/β1′ 2.37	179.4	60.2	β1 26.2/Me β2 24.2/Me γ 7.2	
			Me β2 1.480/Me γ 0.850 (7.5)				
Q[6]	7.938	3.89	β 2.16/β′ 2.25	176.1	58.0	β 27.4/γ 32.6	110.1
			γ 2.38/γ′ 2.531	177.4[a]			101.6[a]
			ε_{anti} 7.438/ε_{syn} 6.753				
U[7]	7.992		Me *pro-R* 1.518/Me *pro-S* 1.572	178.4	58.0	Me *pro-R* 23.2/Me *pro-S* 27.0	122.8
V[8]	7.444	3.62	β 2.29/Me γ1 0.982 (6.7)/Me γ2 1.071 (6.5)	175.2	64.8	β 30.2/Me γ1 19.2/Me γ2 20.2	107.9
U[9]	8.110		Me β1, Me β2 1.456	179.0		Me β1 23.1/Me β2 26.5	124.6
G[10]	8.385	3.67/3.95		173.0	45.0		94.8
L[11]	8.020	4.45	β 1.60/β′ 1.95/γ 1.94	176.1	54.0	β 41.2/γ 25.3	112.7
			Me δ1 0.898 (6.4)/Me δ2 0.919 (6.5)			Me δ1 21.1/Me δ2 23.2	
U[12]	8.260		Me *pro-R* 1.529/Me *pro-S* 1.597	175.2	58.4	Me *pro-R* 26.2/Me *pro-S* 23.7	126.8
P[13]		4.38	β 1.77/β2′ 2.37	176.2	64.5	β 29.7/γ 26.8/δ 50.3	
			γ 1.98/γ′ 2.08				
			δ 3.62/δ′ 3.92				
L[14]	7.901	4.20	β 1.74/β′ 1.91/γ 1.81	176.1	55.3	β 40.1/γ 25.8	109.8
			Me δ1 0.937 (6.5)/Me δ2 1.040 (6.4)			Me δ1 21.3/Me δ2 23.3	
U[15]	7.759		Me β1, Me β2 1.546	177.3		Me β1 23.1/Me β2 26.5	123.9
U[16]	7.602		Me β1, Me β2 1.496	177.8		Me β1 23.2/Me β2 26.4	117.9
Q[17]	7.788	4.04	β β′ 2.05	174.3	56.0	β 28.0/γ 32.9	107.7
			γ 2.36/γ′ 2.25	177.8[a]			101.3[a]
			ε_{anti} 7.346/ε_{syn} 6.715				
Fol[18]	7.484	4.14	β β′ CH_2OH 3.63		54.5	β CH_2OH 64.8	114.6
			β 2.74/β′ 2.96			β 37.7	
			CH_2OH 5.137			Arom. 1′ 139.9/2′, 6′ 130.4	
			Arom. 2′, 6′ 7.282/3′, 5′ 7.216/4′ 7.139			3′, 5′ 129.1/4′ 127.2	

[a] ε ^{15}NH and δ ^{13}CO chemical shifts of glutamine lateral chain.

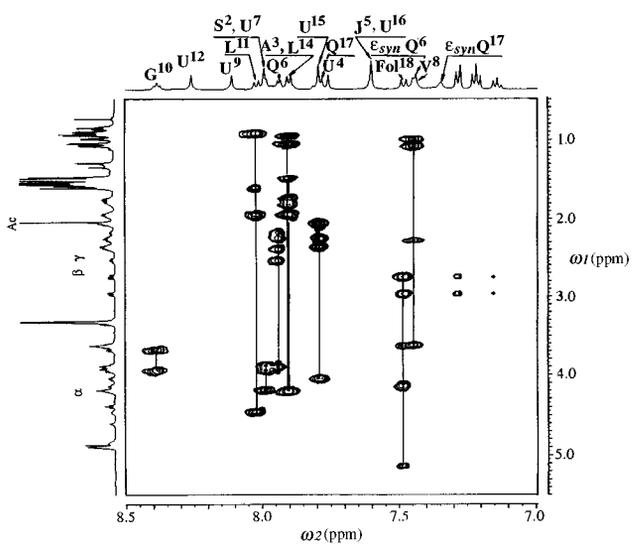

Fig. 4 Part of the TOCSY spectrum of PA VI (CD_3OH; 500.13 MHz; 298 K; spin-lock period 120 ms); $\omega 2$ = 8.5–7.0 ppm, $\omega 1$ = 5.5–0.5 ppm

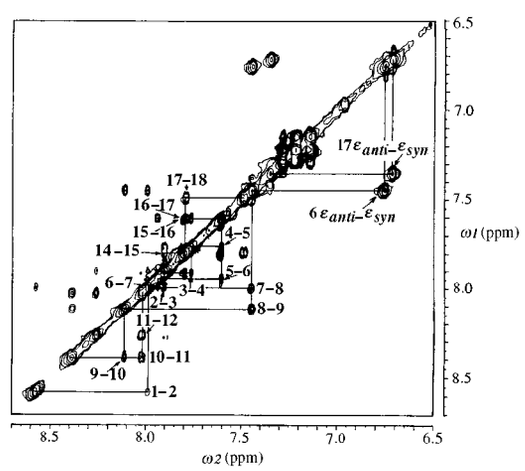

Fig. 5 Part of the ROESY spectrum of PA VI (CD_3OH; 500.13 MHz; 298 K; mixing time 300 ms); $\omega 2$ = 8.7–6.5 ppm, $\omega 1$ = 8.7–6.5 ppm

Hz). Determination of the chemical shifts of each nitrogen, except the proline one, resulted from a ^{1}H–^{15}N HSQC experiment, showing $^{1}J_{NH}$ couplings (Fig. 6). As expected, the ^{15}NH of the α,α-dialkylated Aib residues appeared more deshielded than did those of the Gly and the monoalkylated amino acids.

3 Conformational data

A preliminary study of the NMR solution structure of trichorzins PA was undertaken, in order to examine the influence on the overall secondary structure of Aib/Iva substitutions at positions 4 and 7 in the sequence and of the *C*-terminal Trpol/Pheol replacement. A qualitative analysis of short- and medium-range ROEs, $^{3}J_{NHC\alpha H}$ couplings and H^{α} chemical-shift differences to the random-coil values[27] was used to characterise the secondary structure of trichorzin PA VI. The pattern of $d_{NN(i,\ i+1)}$ and $d_{\alpha N(i,\ i+3)}$ from residues 1 to 18 (Fig. 7) indicated a helical structure all along the sequence, as widely observed for Aib-containing peptides.[28,29] Pro[13] resulted in an interruption of the hydrogen-bonding pattern and might presumably be accommodated in a 3_{10} bend,[9,30] as suggested by the presence of $d_{\alpha N(i,\ i+2)}$ contacts in this part of the helix. Additional support for a helix including some distortion in the 10–14 segment was provided by analysis of the H^{α} chemical shifts.[27] Most of the residues exhibited characteristic helical H^{α} chemical shifts (upfield from their random-coil values, while downfield or null

Table 4 Amide and α-proton chemical shifts (δ, ppm) for trichorzins PA (CD_3OH; 298 K); chemical shifts are given to the nearest three decimals or two decimals when obtained from 1D or 2D spectra, respectively

	PA II		PA IV		PA V		PA VII		PA VIII		PA IX	
Residue	NH	H^{α}	NH	H^{α}	NH	H^{α}	NH	H^{α}	NH	H^{α}	NH	H^{α}
U^{1}	8.591		8.594		8.579		8.587		8.590		8.579	
S^{2}	8.009	4.18	8.00	4.19	7.985	4.20	8.00	4.18	7.995	4.19	8.000	4.20
A^{3}	7.901	4.18	7.93	4.21	7.961	4.17	8.00	4.18	7.984	4.19	7.963	4.18
U^{4} ($J^{4\bullet}$)	7.775		7.750		7.672$^{\bullet}$		7.653$^{\bullet}$		7.745		7.677$^{\bullet}$	
J^{5}	7.613		7.619		7.583		7.590		7.616		7.580	
Q^{6}	7.943	3.90	7.973	3.89	7.961	3.90	8.00	3.89	7.973	3.89	7.963	3.90
ε_{syn}	6.767		6.772		6.780		6.784		6.771		6.773	
ε_{anti}	7.459		7.45		7.465		7.466		7.47		7.459	
U^{7} ($J^{7\bullet}$)	7.999		7.903$^{\bullet}$		7.948		7.861$^{\bullet}$		7.901$^{\bullet}$		7.945	
V^{8}	7.449	3.62	7.445	3.65	7.400	3.64	7.406	3.65	7.441	3.64	7.400	3.65
U^{9}	8.118		8.101		8.098		8.090		8.099		8.096	
G^{10}	8.392	3.66, 3.94	8.337	3.66, 3.93	8.382	3.67, 3.92	8.334	3.67, 3.91	8.342	3.68, 3.93	8.382	3.68, 3.94
L^{11}	8.026	4.46	8.009	4.45	8.011	4.46	8.00	4.44	8.009	4.45	8.011	4.45
U^{12}	8.271		8.235		8.238		8.216		8.232		8.240	
P^{13}		4.38		4.37		4.37		4.37		4.38		4.38
L^{14}	7.885	4.17	7.883	4.15	7.886	4.16	7.878	4.19	7.908	4.21	7.903	4.21
U^{15}	7.775		7.766		7.769		7.771		7.793		7.797	
U^{16}	7.613		7.583		7.584		7.590		7.616		7.615	
Q^{17}	7.811	4.11	7.811	4.09	7.813	4.10	7.816	4.11	7.798	4.04	7.793	4.04
ε_{syn}	6.975		6.737		6.746		6.76		6.723		6.737	
ε_{anti}	7.358		7.347		7.352		7.367		7.355		7.367	
Wol^{18} (Fol^{18}*)	7.555	4.23	7.548	4.23	7.560	4.23	7.557	4.23	7.482*	4.14*	7.490*	4.14*
NH indole$^{\bullet}$	10.188		10.186		10.188							

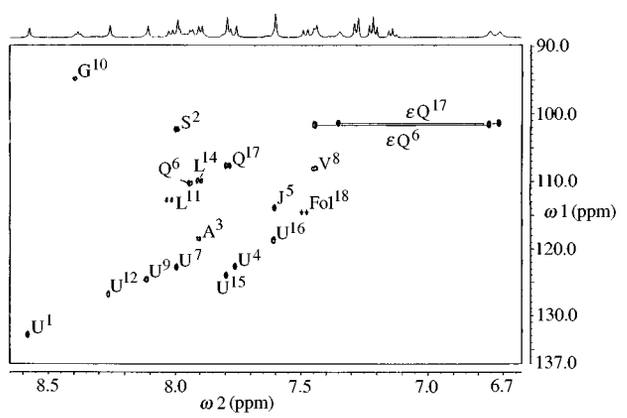

Fig. 6 ^{1}H–^{15}N HSQC spectrum of PA VI (CD_3OH; 50.68 MHz,; 298 K)

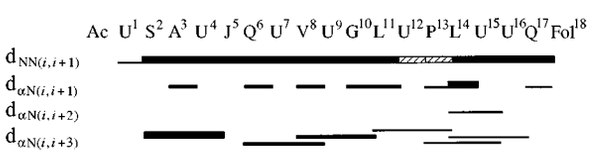

Fig. 7 Summary of the sequential and medium-range ROE connectivities observed for trichorzin PA VI; the height of the bars indicates the strength of the ROEs; the $d_{N\delta}$ connectivities observed for proline are indicated by hatched lines

shifts were noticed for residues 11, 13 and 14 involved in the bend (Fig. 8).

A comparison of the NH and H^{α} chemical shifts (Table 4) and $^{3}J_{NHC\alpha H}$ coupling constants (Table 5), which appeared very homogeneous among the seven trichorzins PA, indicated that they all adopted the same structure. Replacements of Aib for Iva and of Trpol for Pheol resulted systematically in an upfield shift (0.1 ppm) of the concerned amide protons, accompanied in the case of the amino alcohol by a 0.1 ppm upfield shift of the α-proton. All the other residues had very similar NH and H^{α} chemical shifts.

Thus, as previously shown for long-sequence peptaibols, trichorzins PA adopt a helical structure, presumably of the α-type,

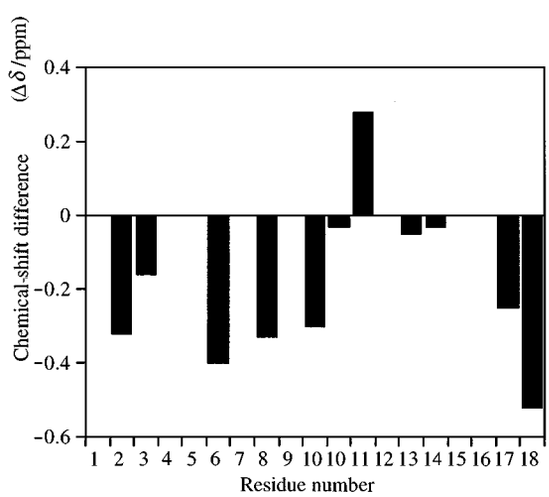

Fig. 8 Chemical-shift differences obtained for the ^{1}H chemical shifts of PA VI α protons to the random coil values

with a distortion in the region including the Pro^{13} residue, which results in a bend in the helix axis. This helical structure is not affected by the Aib/Iva substitutions at positions 4 and 7 or, as expected, by the *C*-terminal Pheol/Trpol replacement. A more detailed conformational study, including molecular modelling under NMR constraints, is now in progress.

Experimental

Isolation of trichorzins PA

A typical 20 l culture of *T. harzianum* (strain M-902608, Laboratoire de Cryptogamie, Muséum National d'Histoire Naturelle, Paris, France) was filtered to separate the mycelium from the culture broth. The filtered broth and wet mycelium were extracted three times with butan-1-ol and methanol, respectively, giving two crude extracts (1.67 g from the broth and 3.63 g from the mycelium), after evaporation to dryness. These extracts were independently submitted first to Sephadex LH 20 chromatography (elution with methanol) and then to silica gel chromatography [SiO_2, Merck; CH_2Cl_2–MeOH (90:10

Table 5 $^3J_{NHC\alpha H}$ coupling constants (Hz) of trichorzins PA

Residue	PA II	PA IV	PA V	PA VI	PA VII	PA VIII	PA IX
S^2	5.5	5.8	5.7	4.9[a]	n.d.	5.5	5.0[b]
A^3	6.3	n.d.	n.d.	4.9[a]	n.d.	5.0	4.8[b]
Q^6	4.8	4.8	n.d.	4.8	4.8	4.8	4.7
V^8	6.3	6.4	6.1	6.3	6.2	6.3	6.3
G^{10}	5.2	5.6	5.4	5.5	5.5	5.7	5.6
	5.2	5.6	5.6	5.5	5.5	5.7	5.6
L^{11}	7.8	n.d.	7.8	7.9	n.d.	7.8	7.6[b]
L^{14}	7.7	7.6	7.5	7.3	7.8	7.2	7.4
Q^{17}	6.9	6.7	6.8	6.5	6.9	6.9	6.9
Wol^{18} (Fol^{18}*)	8.9	9.1	9.0	9.2*	9.4	9.2*	9.4*

[a,b] Determined at 311 K and 278 K, respectively; n.d., not determined from the 1D spectra due to severe superimposition of the signals.

to 0:100)]. Trichorzins PA (347 mg from the broth and 127 mg from the mycelium) were eluted with CH_2Cl_2–MeOH (80:20) and visualised on thin-layer chromatograms [SiO_2, Merck 60 F 254; CH_2Cl_2–MeOH (70:30)] by spraying with anisaldehyde reagent [anisaldehyde–H_2SO_4–AcOH (1:1:50)]. Further HPLC analyses showed the same trichorzins PA composition for the two microheterogeneous mixtures arising from culture broth and mycelium.

HPLC separation of trichorzins PA

The HPLC separation was carried out with a Waters liquid chromatograph: 600 Controller, 717 Autosampler and 486 Tunable absorbance detector, on a semi-preparative reversed-phase Kromasil C_{18} column (300 × 7.5 mm, AIT France) with MeOH–water (84:16) as eluent and a flow rate of 2 cm^3 min^{-1}; t_R (min) PA I: 58, PA II: 74, PA III: 81, PA IV: 89, PA V: 95, PA VI: 106, PA VII: 111, PA VIII: 127, PA IX: 136. Purity of the isolated peptides was checked by HPLC on an analytical Kromasil C_{18} column (250 × 4.6 mm, AIT France) with MeOH–water (83.4:16.6) as eluent and a flow rate of 1 cm^3 min^{-1}.

Amino acid composition

Hydrolysis and derivatisation. 1 mg of each trichorzin was hydrolysed according to the general procedure (6 mol dm^{-3} HCl; 110 °C; Ar; 24 h) in a sealed tube. The residue was evaporated to dryness under vacuum in the presence of NaOH pellets. Crude amino acid and amino alcohol mixtures were derivatised by adding 1 cm^3 of 3 mol dm^{-3} HCl in propan-2-ol (100 °C; 30 min). After removal of solvent under reduced pressure, 0.5 cm^3 of CH_2Cl_2 and 0.5 cm^3 of trifluoroacetic anhydride were added (100 °C; 10 min). After removal of the reagents, the derivatives were dissolved in CH_2Cl_2 and submitted to GLC analysis. For Trpol characterisation, the peptides were hydrolysed under mild acidic conditions, in the presence of 3 mol dm^{-3} mercaptoethanesulfonic acid (sealed tubes under vacuum; 110 °C; 24 h). The mixture was then neutralised (3 mol dm^{-3} NaOH), and evaporated under reduced pressure. The residue was derivatised as described above.

GLC analysis of *N*-trifluoroacetylated isopropyl ester derivatives. GLC analyses of the derivatives were performed on a Hewlett Packard series II 5890 gas chromatograph on a Chirasil-L-Val (*N*-propionyl-L-valine-*tert*-butylamide polysiloxane) quartz capillary column (Chrompack, 25 m length, 0.2 mm i.d.), with He (0.7 bar) as carrier gas and a temperature programme: 50 ⟶ 130 °C, 3 °C min^{-1}; 130 ⟶ 190 °C, 10 °C min^{-1}.

t_R (min)-values (separation factor $\alpha_{L/D}$ for the D-L amino acid and amino alcohol enantiomers): Aib 6.75, L-Ala 10.61 (α 1.20), L-Glu 29.42 (α 1.02), Gly 13.14, D-Iva 7.36 (α 1.02), L-Leu 19.10 (α 1.13), L-Pheol 29.48 (α 0.94), L-Pro 16.38 (α 1.01), L-Ser 18.16 (α 1.07), L-Trpol 40.42 (α 0.99), L-Val 13.11 (α 1.13).

Amino acid composition and absolute configuration for trichorzins PA:

PA II: Aib (7), L-Ala (1), L-Gln (2), Gly (1), D-Iva (1), L-Leu (2), L-Pro (1), L-Ser (1), L-Trpol (1), L-Val (1)
PA IV: Aib (6), L-Ala (1), L-Gln (2), Gly (1), D-Iva (2), L-Leu (2), L-Pro (1), L-Ser (1), L-Trpol (1), L-Val (1)
PA V: Aib (6), L-Ala (1), L-Gln (2), Gly (1), D-Iva (2), L-Leu (2), L-Pro (1), L-Ser (1), L-Trpol (1), L-Val (1)
PA VI: Aib (7), L-Ala (1), L-Gln (2), Gly (1), D-Iva (1), L-Leu (2), L-Pheol (1), L-Pro (1), L-Ser (1), L-Val (1)
PA VII: Aib (5), L-Ala (1), L-Gln (2), Gly (1), D-Iva (3), L-Leu (2), L-Pro (1), L-Ser (1), L-Trpol (1), L-Val (1)
PA VIII: Aib (6), L-Ala (1), L-Gln (2), Gly (1), D-Iva (2), L-Leu (2), L-Pheol (1), L-Pro (1), L-Ser (1), L-Val (1)
PA IX: Aib (6), L-Ala (1), L-Gln (2), Gly (1), D-Iva (2), L-Leu (2), L-Pheol (1), L-Pro (1), L-Ser (1), L-Val (1).

LSI Mass spectrometry

Positive-ion liquid secondary-ion mass spectra were recorded on a VG analytical ZAB-2 SEQ mass spectrometer (VG Analytical, Manchester, UK), equipped with a standard FAB source and a caesium ion gun operating at 35 kV. Peptide samples dissolved in methanol were mixed with the matrix, either α-thioglycerol, 3-nitrobenzyl alcohol or 3-nitrobenzyl alcohol saturated with LiCl. The resolution was about 1000.

NMR spectroscopy

A 0.5 cm^3 amount of 5–20 10^{-3} mol dm^{-3} methanolic (CD_3OH) peptide solution in a 5 mm tube (Wilmad) was used for the NMR experiments, which were conducted at 298 K unless otherwise specified. Spectra were recorded either on an AC 300 or a DMX 500 Bruker spectrometer, equipped with Aspect 3000 and Avance 500 station 1 computers, respectively. ^1H Spectra were referenced to the central signal of the quintuplet due to the CD_2H resonance of methanol at δ 3.313, downfield from $SiMe_4$ (TMS). ^1H 1D COSY experiments were recorded at 300 MHz, with solvent presaturation. TOCSY and ROESY experiments were recorded at 500 MHz, with solvent signal suppression by the WATERGATE scheme included in the pulse sequences, with a mixing time of 120 ms and 250 ms, respectively. ^{13}C Spectra were referenced to the central signal of methanol at δ_C 49.0, downfield from TMS. ^1H–^{13}C HSQC and HMBC experiments were optimised for ^1H–^{13}C coupling constants of 135 and 5 Hz, respectively. The ^1H–^{15}N HSQC experiment was referenced from formamide in 10% [$^2H_6$]-acetone, at 112.4 ppm, downfield to NH_3, used as secondary external reference.[31] The ^{13}C and ^{15}N 2D spectra were processed using sine-bell squared functions in F1 and F2 dimensions shifted by 6-2, 2-2 and 6-2, respectively.

Antibiotic assays with mycoplasmas

Antibiotic activity of trichorzins PA was checked against different mollicutes: *Mycoplasma gallisepticum*, *M. mycoides* sp. *mycoides*, *Spiroplasma citri*, *Sp. apis*, *Sp. floricola* BNR1, *Sp. melliferum* and *Acholeplama laidlawii*, as described previously.[17]

Briefly, the mollicutes at 10^6 colony-forming units (CFU) dm^{-3} were grown for 48 h under microaerobic conditions, in appropriate liquid media and in the presence of trichorzin concentrations ranging between 0 and 100 μmol dm^{-3}. Minimum inhibitory concentrations (MICs) were determined in 96-well microtitration plates by following the colour change of Phenol Red, resulting from acidification of the culture medium during the cell growth. The MIC-values obtained were between 3 and 25 μM.

Acknowledgements

We thank Pr. M. F. Roquebert (Laboratoire de Cryptogamie, Muséum National d'Histoire Naturelle, Paris) for kindly providing the *Trichoderma harzianum* strain, Pr. H. Wroblewski and L. Beven (URA 256, GDR 1153 CNRS, Université de Rennes I) for the measurements on mycoplasmas, and Dr. J. P. Brouard (Laboratoire de Chimie des Substances Naturelles, Muséum National d'Histoire Naturelle, Paris) for his help in the GLC analyses. The 500 MHz facilities used in this study were funded by the Région Haute-Normandie, France.

References

1 R. C. Pandey, J. C. Cook, Jr. and K. L. Rinehart, Jr., *J. Am. Chem. Soc.*, 1977, **99**, 8469.
2 P. Mueller and D. O. Rudin, *Nature*, 1968, **217**, 713.
3 M. S. P. Sansom, *Q. Rev. Biophys.*, 1993, **26**, 365.
4 M. El Hajji, S. Rebuffat, T. Le Doan, G. Klein, M. Satre and B. Bodo, *Biochim. Biophys. Acta*, 1989, **978**, 97.
5 G. Baumann and P. Mueller, *J. Supramol. Struct.*, 1974, **2**, 538.
6 G. Boheim, *J. Membr. Biol.*, 1974, **19**, 277.
7 G. Jung, W. A. König, D. Leibfritz, T. Ooka, K. Janko and G. Boheim, *Biochim. Biophys. Acta*, 1976, **45**, 164.
8 B. Bodo, S. Rebuffat, M. El Hajji and D. Davoust, *J. Am. Chem. Soc.*, 1985, **107**, 6011.
9 S. Rebuffat, Y. Prigent, C. Auvin-Guette and B. Bodo, *Eur. J. Biochem.*, 1991, **201**, 667.
10 I. L. Karle, J. L. Flippen-Anderson, S. Agarwalla and P. Balaram, *Proc. Natl. Acad. Sci. USA*, 1991, **88**, 5307.
11 S. Rebuffat, C. Goulard and B. Bodo, *J. Chem. Soc., Perkin Trans. 1*, 1995, 1849.
12 S. Rebuffat, S. Hlimi, Y. Prigent, C. Goulard and B. Bodo, *J. Chem. Soc., Perkin Trans. 1*, 1996, 2021.
13 C. Auvin-Guette, S. Rebuffat, Y. Prigent and B. Bodo, *J. Am. Chem. Soc.*, 1992, **114**, 2170.
14 T. Fujita, S. Wada, A. Iida, T. Nishimura, M. Kanai and N. Toyama, *Chem. Pharm. Bull.*, 1994, **42**, 489.
15 S. Razin, *Microbiol. Rev.*, 1978, **42**, 414.
16 S. Razin, *FEMS Microbiol. Lett.*, 1992, **100**, 423.
17 L. Beven, M. Le Hénaff, C. Fontenelle and H. Wroblewski, *Curr. Microbiol.*, 1996, **33**, 317.
18 H. R. Morris and M. Panico, *Biochem. Biophys. Res. Commun.*, 1981, **101**, 623.
19 R. Roepstorff, P. Horjrup and J. Moller, *Biomed. Mass Spectrom.*, 1985, **12**, 181.
20 K. Biemann, *Biomed. Environ. Mass Spectrom.*, 1988, **16**, 99.
21 M. El Hajji, S. Rebuffat, D. Lecommandeur and B. Bodo, *Int. J. Pept. Protein Res.*, 1987, **29**, 207.
22 H. Brückner and M. Przybylski, *J. Chromatogr.*, 1984, **296**, 263.
23 M. Becchi, S. Rebuffat, J. Y. Dugast, S. Hlimi, B. Bodo and G. Molle, *Rapid Commun. Mass Spectrom.*, 1995, **9**, 37.
24 R. P. Grese, R. L. Cerny and M. L. Gross, *J. Am. Chem. Soc.*, 1989, **111**, 2835.
25 L. M. Teesch and J. Adams, *J. Am. Chem. Soc.*, 1991, **113**, 812.
26 K. Wüthrich, *NMR of Proteins and Nucleic Acids*, Wiley, New York, 1986.
27 D. S. Wishart, B. D. Sykes and F. M. Richards, *Biochemistry*, 1992, **31**, 1647.
28 I. L. Karle and P. Balaram, *Biochemistry*, 1990, **29**, 6747.
29 C. Toniolo and E. Benedetti, *TIBS*, 1991, **16**, 350.
30 G. Esposito, J. A. Carver, J. Boyd and I. D. Campbell, *Biochemistry*, 1987, **26**, 1043.
31 P. R. Srinivasan and R. Lichter, *J. Magn. Reson.*, 1977, **28**, 227.

Paper 7/00244K
Received 10*th January* 1997
Accepted 24*th March* 1997